APPLIED ORGANOMETALLIC CHEMISTRY
Appl. Organometal. Chem. **13**, 565–581 (1999)

Dinuclear Cyclopalladated Azobenzene Complexes: a Comparative Study on Model Compounds for Organometallic Liquid-Crystalline Materials

Mauro Ghedini,[1]* Daniela Pucci,[1] Alessandra Crispini,[1] Iolinda Aiello,[1] Francesco Barigelletti,[2] Alessandro Gessi[2] and Oriano Francescangeli[3]

[1]Dipartimento di Chimica, Università della Calabria, I-87030 Arcavacata (CS), Italy
[2]Istituto FRAE-CNR, Via P. Gobetti 101, I-40129 Bologna, Italy
[3]Dipartimento di Scienze dei Materiali and Istituto Nazionale per la Fisica della Materia, Università di Ancona, Via Brecce Bianche, I-60131 Ancona, Italy

The series of dinuclear 4,4′-bis(hexyloxy)azobenzene, [H(Azo-6)], cyclopalladated complexes of general formula [Azo-6)Pd(μ-X)]$_2$, (X = Cl, Br, I, N_3, SCN, OAc) and [Azo-6)$_2$Pd$_2$(μ-Ox)] (Ox = oxalate) have been synthesized and investigated for mesomorphism and spectroscopic properties. Single-crystal X-ray analysis of the dinuclear bromo- and iodo-bridged complexes has been performed. The structural data, compared with those of the known homologous chloro compound, show that all the [Azo-6)Pd(μ-X)]$_2$)] (X = Cl, Br, I) molecules crystallize in the monoclinic space group $P2_1/c$ and are isomorphous. They are arranged in slipped pairs with intermolecular non-bonding Pd–Pd contacts ranging from 3.668(1) Å(X = Cl) to 3.758(3) Å(X = I). The different nature of the bridging group allows variation of the distance between the palladium atoms and the bond environment experienced by the metal centers. Thus, this comparative study reveals that the effectiveness of the bridging group in promoting thermotropic mesophases is greater for chloride, bromide, azide or oxalate than for iodide, thiocyanate or acetate. The greatest range of liquid-crystal behavior was displayed by [Azo−6)$_2$Pd$_2$(μ−Ox)]. Remarkably, this compound is the first example of a metallomesogen containing the bridging oxalate group.

The bimetallic complexes exhibit different absorption spectra (i.e. colors) depending, in general terms, on the nature of the bridge connecting the two cyclometalated [H(Azo-6)] moieties, which can be varied so as to tune the optical properties. Blocking the azo group in the *trans* position results in several cases in weakly luminescent complexes, with luminescence efficiencies $\phi \approx 10^{-4}$ and luminescence lifetimes of the order of nanoseconds.

Using the data obtained from the 4,4′-bis(hexyloxy)azoxybenzene [H(Azoxy-6)] derivative, [Azoxy-6)Pd(μ-Cl)]$_2$, from the mononuclear acetylacetonate (acac) complexes [(Azo-6)Pd(acac)] and [(Azoxy-6)Pd(acac)], and from the uncomplexed [H(Azo-6)] and [H(Azoxy-6)] ligands, the nature of the excited states relevant to the photophysical behavior are discussed.

Keywords: azocompounds; cyclopalladated complexes; luminescence; X-ray structure; metallomesogens

Received 4 December 1998; accepted 22 February 1999

* Correspondence to: Professor Mauro Ghedini, Dipartimento di Chimica, Università della Calabria, I-87030 Arcavacata (CS), Italy. E-mail: m.ghedini@unical.it
Contract/grant sponsor: Ministero per l'Università e la Ricerca Scientifica e Tecnologica (MURST).
Contract/grant sponsor: Consiglio Nazionale della Ricerche (CNR).
Contract/grant sponsor: Regione Calabria (POP 1994–99).

 CCC 0268–2605/99/080565–17 $17.50

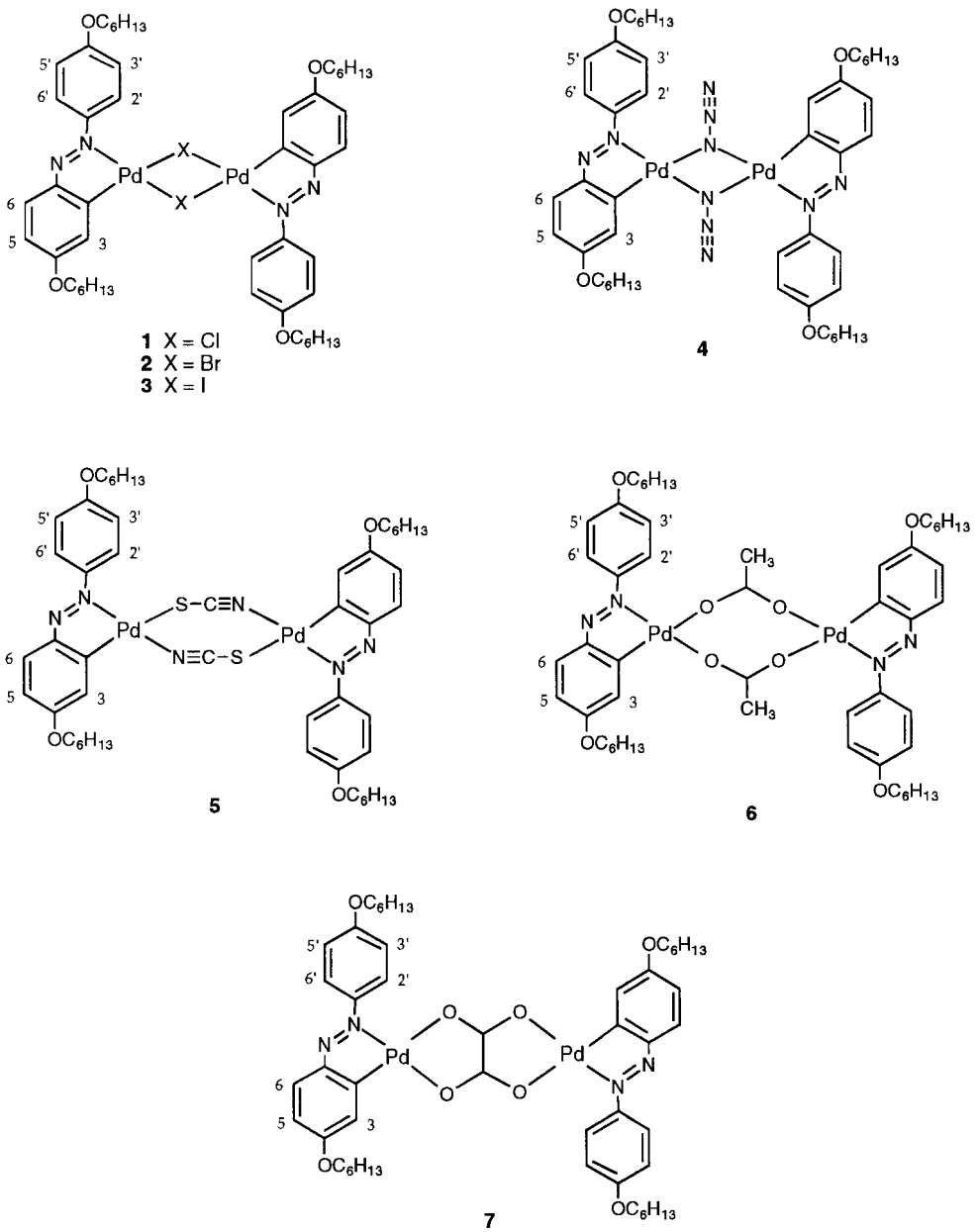

Figure 1 General formulae and aromatic proton numbering schemes of the dinuclear complexes [(Azo-6)Pd(μ-X)]$_2$, (**1–6**: X = Cl, Br, I, N_3, SCN, OAc, respectively) and [(Azo-6)$_2$Pd$_2$(μ-Ox)], **7**.

INTRODUCTION

Liquid-crystalline compounds are self-assembling species whose anisotropic properties are suitable for applications in electro-optical devices which require fluid materials or thin solid films.[1,2] In the former case the molecules undergo reorientation by the effect of an applied field whereas in the latter no molecular switching is involved. Recent developments in optical materials based on these different mechanisms include the enhanced photorefractivity observed in nematic liquid crystals properly doped

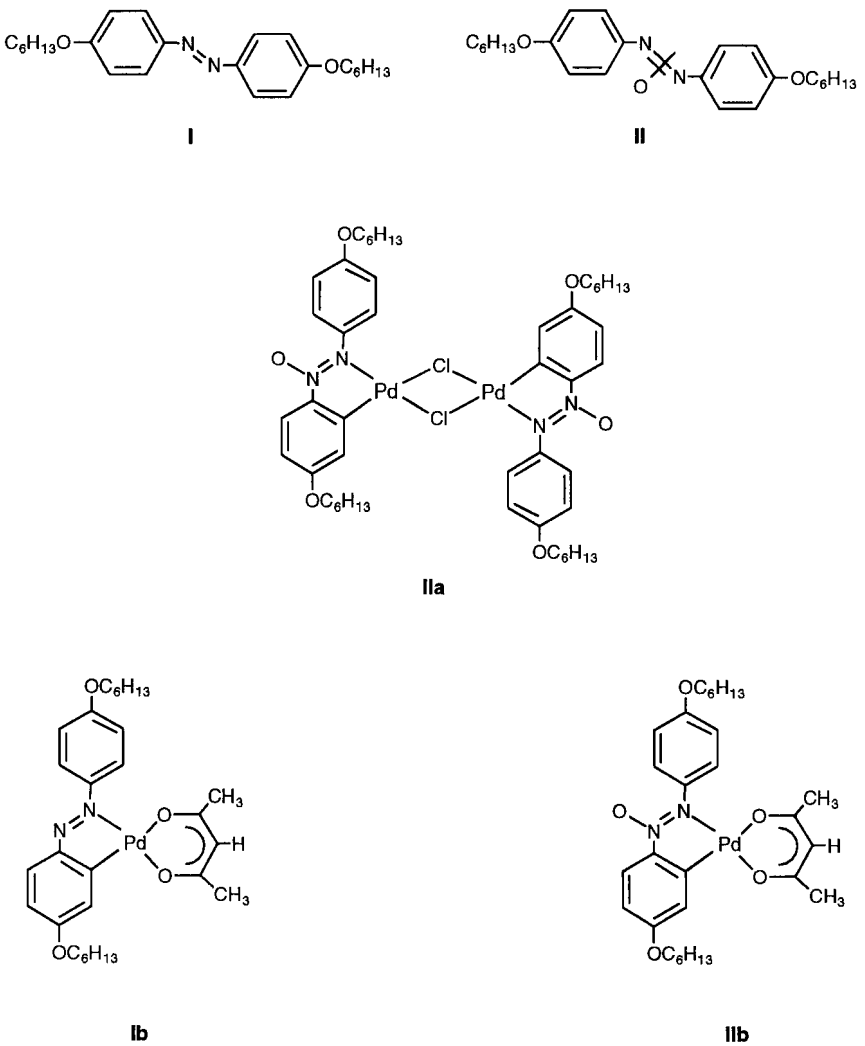

Figure 2 General formulae and aromatic proton numbering schemes of the reference compounds **I, II, IIa, Ib** and **IIb**.

with electron donor–acceptor molecules[3] and the increased luminescence properties displayed by ordered films obtained by vitrifiable liquid crystals.[4,5] The synthesis of mesogenic materials should be accurately planned according to the selected technological approach, and the target of the present investigation is to explore new synthesis routes to produce organometallic compounds able to form long-term stable and well-organized mesophases.

The dinuclear cyclopalladated complexes are a well-known class of metallomesogens featuring an 'H-shaped' molecular structure.[6] These species, when they contain appropriate azobenzene ligands, afford high-viscosity fluid phases[7,8] and in solution may be weakly luminescent.[9] In particular, the chloro-bridged dimer $[(\text{Azo-6})\text{Pd}(\mu\text{-Cl})]_2$ (**1** in Fig. 1) obtained by *ortho*-palladation of 4,4′-bis(hexyloxy)azobenzene, [H(Azo-6)], has revealed interesting characteristics in terms of crystal packing and mesomorphism.[8] A dichloromethane solution of this complex exhibits absorption maxima at 258, 375 and 472 nm (with extinction coefficients $\varepsilon = 32000$, 22000 and 22000 $\text{M}^{-1}\,\text{cm}^{-1}$ respectively) and a luminescence band maximum at 536 nm ($\phi = 0.9 \times 10^{-4}$, $\tau = 3.4$ ns).[9b]

We wished to attain the possibility of tuning both the mesomorphic and spectroscopic properties of

these systems. In particular, we hoped to change the nature of the bridging ligands so as to modulate, through the distance between the palladium centers, the anisometric ratio between molecular length and width and the bond environment of the metal centers. To this aim, as useful models, we have taken into account the series of dinuclear ortho-palladated [H(Azo-6)] derivatives, [(Azo-6)Pd(μ-X)]$_2$, (**1–6**: X = Cl, Br, I, N_3, SCN, OAc respectively) and [(Azo-6)$_2$Pd$_2$(μ-Ox)] (**7**: Ox = oxalate), shown in Fig. 1.

In this paper we describe the synthesis, the characterization and the mesomorphic, spectroscopic and photophysical properties of such a family of homologous complexes. Moreover, as far as the spectroscopic data are concerned, the results obtained are compared with those of the related dinuclear cyclopalladated, chloro-bridged complex [(Azoxy-6)Pd(μ-Cl)]$_2$, **IIa**, arising from 4,4′-bis-(hexyloxy)azoxybenzene, [H(Azoxy-6)], of the mononuclear acetylacetonate (acac) derivatives, [(Azo-6)Pd(acac)], **Ib**, and [(Azoxy-6)Pd (acac)], **IIb**, and of the uncomplexed ligands [H(Azo-6)], **I**, and [H(Azoxy-6)], **II** (Fig. 2).

EXPERIMENTAL

General procedure and instruments

^{1}H-NMR ($CDCl_3$ solutions, Me_4Si internal standard) and infrared spectra (KBr pellets) were recorded on a Bruker WM-300 and on a Perkin-Elmer 2000 FT-IR spectrometer, respectively. Elemental analyses were performed with a Perkin-Elmer 2400 analyzer.

The optical observations were made with a Zeiss Axioskop polarizing microscope equipped for photography and with a Linkam CO 600 heating stage. Transition temperatures and enthalpies were obtained by a Perkin-Elmer DSC-7 differential scanning calorimeter (DSC) with heating and cooling rates of 10 °C min^{-1}. The X-ray powder diffraction (XRD) measurements were performed with an INEL CPS-120 powder diffractometer using monochromatized $Cu_{K\,\alpha}$ radiation λ = 1.54 Å).

Room-temperature absorption and luminescence spectra of aerated dichloromethane solutions were recorded with a Perkin-Elmer Lambda 5 spectrometer and with a Spex Fluorolog II spectrofluorimeter, respectively. Excitation spectra were also obtained and found to match the absorption profiles. Uncorrected luminescence band maxima are used throughout the text. In order to determine luminescence quantum yields we obtained luminescence spectra by employing isoabsorbing solutions at λ_{exc} 450 nm. Correction of the spectra for the phototube response was then accomplished and we compared the areas under the corrected luminescence profiles on an energy scale (cm^{-1}) with that for $[Ru(bpy)_3]^{2+}$ (ϕ = 0.028) in aerated water solution; the experimental procedure is described in a previous paper.[10] The experimental uncertainty in the band maxima is 2 nm while that for the luminescence intensity is 20%. Luminescence lifetimes were obtained with an IBH single-photon equipment (N_2 lamp, excitation at 337 nm). The uncertainty on the evaluated lifetimes is 10%.

Synthesis

All chemicals and the ligand [H(Azoxy-6)], **II** (Kodak), were used without further purification. The ligands [H(Azo-6)], **I**,[8] the chloro-bridged dinuclear complex [(Azo-6)Pd(μ-Cl)]$_2$, **1**,[8] and the reference compounds [(Azo-6)Pd(acac)], **Ib**,[11] [(Azoxy-6)Pd(μ-Cl)]$_2$, **IIa**,[11] and [(Azoxy-6)Pd (acac)], **IIb**,[11] were prepared as reported elsewhere.

[(Azo-6)Pd(μ-Br)]$_2$ 2
A 20-fold excess of NaBr (294 mg, 2.86 mmol) was added to a suspension of **1** (150 mg, 0.14 mmol) in acetone (5 ml) and the mixture was stirred at room temperature for 24 h. After removal of the solvent under reduced pressure, the crude product was dissolved in chloroform and extracted with water. The organic layer was then dried over anhydrous sodium sulfate and the chloroform evaporated under reduced pressure to give a pale brown solid in 85% yield (122 mg). Analysis: Calcd: C, 50.76; H, 5.85; N, 4.39. Found: C, 50.86; H, 5.74; N, 4.35%.

[(Azo-6)Pd(μ-I)]$_2$ 3
A suspension of **1** (150 mg, 0.14 mmol) and a 20-fold excess of KI (475 mg, 2.86 mmol) in 5 ml of acetone was stirred in the dark for 6 h. The so-formed red solid was filtered off, washed with water, recrystallized from chloroform–ethanol and dried under vacuum. Yield: 141 mg (80%). Analysis: Calcd: C, 46.88; H, 5.40; N, 4.56. Found: C, 46.50; H, 5.39; N, 4.93%.

[(Azo-6)Pd(μ-N$_3$)]$_2$ 4
A solution of **1** (100 mg, 0.095 mmol) in dichloromethane (15 ml) was added to a 20-fold excess of NaN_3 suspended in acetone (15 ml). The mixture

was stirred at room temperature for 24 h, then the white precipitate (salt) was filtered off and the solvent was evaporated to leave an orange solid which was recrystallized from acetone. Yield: 91 mg (90%). Analysis: Calcd: C, 54.39; H, 6.28; N, 13.18. Found: C, 53.77; H, 6.11; N, 13.18%. IR (KBr): 2071 cm^{-1} (N_3).

[(Azo-6)Pd(μ-SCN)]$_2$ 5
A mixture of **1** (150 mg, 0.14 mmol) and KSCN (280 mg, 2.86 mmol) in acetone (5 ml) was stirred at room temperature overnight and the solvent was then evaporated off. The resulting red solid was dissolved in dichloromethane and extracted with water; the organic layer was dried over anhydrous sodium sulfate and evaporation of the dichloromethane gave a red solid which was filtered off, washed with chloroform and dried *in vacuo*. Yield: 94 mg (60%). Analysis: Calcd: C, 54.99; H, 6.09; N, 7.69. Found: C, 54.08; H, 5.97; N, 7.87%. IR (KBr): 2148 cm^{-1}(SCN).

[(Azo-6)Pd(μ-OAc)]$_2$ 6
Palladium acetate (35 mg, 0.16 mmol) was added to a suspension of an equimolar amount of [H(Azo-6)] (60 mg) in 30 ml of acetic acid and the stirred mixture was kept at 50 °C for 2.5 h. The violet precipitate was filtered off and recrystallized from diethyl ether. Yield: 77 mg (90%). Analysis: Calcd: C, 57.09; H, 6.63; N, 5.12. Found: C, 56.96; H, 6.55; N, 5.10%. IR (KBr): 1592 cm^{-1} (C═O).

[(Azo-6)$_2$Pd$_2$(μ-Ox)] 7
This compound was synthesized following two different procedures: (a) starting from the chloro-bridged derivative **1** by a metathetical reaction with sodium oxalate; and (b) reacting the acetate-bridged complex **6** with oxalic acid.

Procedure (a)
$[Na(OX)]_2$ (380 mg, 2.86 mmol) was dissolved in water (2 ml) and added to a suspension of **1** (150 mg, 0.14 mmol) in acetone (5 ml). The resulting mixture was stirred at room temperature for three days and the dark red solid formed was recovered by filtration, washed with water, recrystallized from chloroform–ethanol and dried under reduced pressure to give a red product in 90% yield (137 mg). Analysis: Calcd: C, 56.44; H, 6.25; N, 5.26. Found: C, 56.00; H, 6.14; N, 4.95%. IR (KBr): 1636 cm^{-1} (C═O).

Procedure (b)
To a suspension of **6** (100 mg, 0.09 mmol) in ethanol (5 ml) an equimolar amount of oxalic acid (11 mg) was added; the suspension turned immediately from violet to red–orange. The mixture was then stirred at room temperature for 1.5 h. The red solid was filtered off, washed with water and ethanol and dried under vacuum. Yield: 92 mg (95%). Analysis: Calcd: C, 56.44; H, 6.25; N, 5.26. Found: C, 56.20; H, 6.15; N, 5.19%. IR (KBr): 1635 cm^{-1} (C═O).

X-ray structure determination and refinement of complexes 2 and 3

The complexes **2** and **3** were recrystallized from chloroform. An orange crystal of **2** (0.22 mm × 0.44 mm × 0.48 mm) and a red crystal of **3** (0.23 mm × 0.08 mm × 0.20 mm) were used for data collection. X-ray data were collected on a Siemens R3m/V four-circle diffractometer, using $Mo_{K\alpha}$ radiation λ = 0.71073 Å).

Corrections were applied for Lorentz and polarization effects. Absorption corrections were applied by using the ψ-scan method for both data collections.[12] Both structures were solved by Patterson methods and completed by Fourier recycling. The refinement was performed using a full-matrix least-squares procedure minimizing the function $\sum \omega (|F_o| - |F_c|)^2$. The weighting scheme used in the last refinement cycle was $\omega^{-1} = \sigma^2 |F_o| + q| F_c|^2$, with q = 0.0001 for **2** and q = 0.0012 for **3**. Anisotropic displacement parameters were introduced only for Pd, Br, I, N and O atoms. The hydrogen atoms were included as idealized atoms riding on the respective carbon atoms with C–H bond lengths appropriate to the carbon atom hybridization. The isotropic displacement parameters of each hydrogen atom were fixed at U = 0.08 Å^2. In both cases, some disorder was found in two of the aliphatic chains [from C(30) to C(36) and from C(43) to C(48)]. The refinement was carried out using geometric constraints for the carbon atoms (the C–C distances were assumed to be 1.53 Å). All calculations were performed with SHELXTL PLUS[13] and PARST[14] programs. Atomic scattering factors were as implemented in the SHELXTL PLUS program.

RESULTS AND DISCUSSION

Synthesis

The cyclopalladated dinuclear complexes [(Azo-

Table 1 Selected ^{1}H-NMR data for complexes **1**–**7** [δ (ppm), multiplicities][a]

H	**1**[b]	**2**	**3**	**4**	**5**	**6**	**7**
$H^{2'}$, $H^{6'}$	7.76 (d)	7.71 (d)	7.66 (d)	7.79 (d)	7.80 (d)	7.30 (d)	7.98 (d)
H^3	6.83 (s)	7.02 (d)	7.36 (d)	6.60 (d)	6.45 (d)	5.89 (d)	6.78 (s)
$H^{3'}$, $H^{5'}$	6.91 (d)	6.92 (d)	6.93 (dd)	6.96 (dd)	6.96 (dd)	6.68 (d)	6.94 (dd)
H^6	7.70 (d)	7.76 (d)	7.82 (d)	7.77 (d)	7.77 (d)	7.54 (d)	7.63 (d)
H^5	6.68 (dd)	6.69 (dd)	6.70 (dd)	6.75 (dd)	6.69 (dd)	6.59 (dd)	6.66 (dd)

[a] Spectra recorded in $CDCl_3$ at 300 MHz; s, singlet; d, doublet.
[b] Ref. 8.

6)Pd(μ-X)]$_2$, **2–5**, were readily obtained, by metathetical reactions, treating the chloro-bridged compound **1** with the appropriate MX salts, whereas the reaction between the ligand **l** and an equimolar amount of palladium(II) acetate gave the cyclopalladated dinuclear acetate-bridged complex [(Azo-6)Pd(μ-OAc)]$_2$, **6**. The oxalate-bridged species **7** was obtained in similar yields by exchange reactions starting either from **1** and sodium oxalate or from **6** and oxalic acid. The formation of **7** was faster from **6** than from **1** (Experimental section).

All the new synthesized complexes display analytical data which are in full agreement with the proposed stoichiometries (Experimental section) and have been characterized by IR and ^{1}H-NMR spectroscopies (Table 1). In particular, regarding the ^{1}H-NMR signals, attention was focused on the proton H^3 (Fig. 1) since the frequency at which it resonates proved very sensitive to the nature of the palladium-bonded bridging groups. The H^3 signal is indeed at 6.83 ppm for **1** while it appears to be shifted downfield by 0.19 and 0.53 ppm for **2** and **3**, respectively.

The IR spectrum of [(Azo-6)Pd(μ-N_3)]$_2$, **4**, shows a strong band at 2071 cm^{-1} which can be assigned to the asymmetric N_3 stretching vibration of a μ-(1,1)-azide-bridged group.[15] Thus, as previously observed in similar dinuclear palladium complexes, the two N_3 ligands form a four-membered Pd_2N_2 ring as shown in Fig. 1 (Ref. 16; see also A. Crispini and M. Ghedini, Comments Inorg. Chem. (1999), in press). The H^3 proton of **4** resonates at 6.60 ppm, shifted upfield (0.23 ppm) with reference to the homologous signal of **1**, possibly because it is shielded by the azide group.

The complex [(Azo-6)Pd(μ-SCN)]$_2$, **5**, is distinguished by an absorption in the IR spectrum at 2148 cm^{-1}, diagnostic of a thiocyanate bridging group.[17] The ^{1}H NMR spectrum of **5** shows the H^3 signal at 6.45 ppm, shifted upfield ($\Delta\,\delta$ = 0.38 ppm) with respect to **1**, by the effect of the anisotropic magnetic field exerted by the π-electrons in the thiocyanate-bridging group.[18] Moreover, the ^{1}H NMR signals reveal the presence of only one isomer; therefore, according to the usual antisymbiotic behavior of palladium compounds, it is suggested that the two thiocyanate-bridging groups are antiparallel to each other.[19] The molecular structure proposed for **5** is depicted in Fig. 1.

The acetate compound **6**, [(Azo-6)Pd(μ-OAc)]$_2$, gives an IR spectrum wherein the absorptions which could be attributed to the acetate groups cannot be assigned because they are superimposed on those arising from the azobenzene ligands. However, in the ^{1}H-NMR spectrum, one singlet (2.09 ppm) accounting for the two CH_3COO groups is detected. Hence, of the two possible diastereoisomers (*cis* and *trans*) only the *trans*, for which the methyl groups are equivalent, is formed. Moreover, as previously observed for like compounds,[18,20] three different triplets (δ = 3.47, 3.73 and 3.95 ppm respectively), which result from the diastereotopic methylenic protons of the alkoxy chains, are present. The ^{1}H-NMR signal corresponding to the H^3 proton shows a strong upfield shift (0.94 ppm) with respect to the values obtained for **1**. This shift could result from the anisotropic magnetic field created by the *ortho*-palladated ring of the other ligand.[18,21] Therefore, for the molecular structure of **6** a strongly bent geometry, 'open-book'-shaped, as obtained by X-ray analysis of related complexes, is proposed (Ref. 21; see also A. Crispini and M. Ghedini, Comments Inorg. Chem. (1999), in press).

The IR spectrum of [(Azo-6)$_2$Pd$_2$(μ-Ox)], **7**, shows a peak, centered at 1636 cm^{-1} [ν_{as}(CO)], characteristic of a tetradentate oxalate bridge,[22] while other bands appear overlapped with those of the azobenzene skeletons. The H^3 signal in the protonic spectrum is found at 6.78 ppm, only weakly shifted upfield (0.05 ppm) with respect to **1**. On the basis of this evidence, for this complex, it

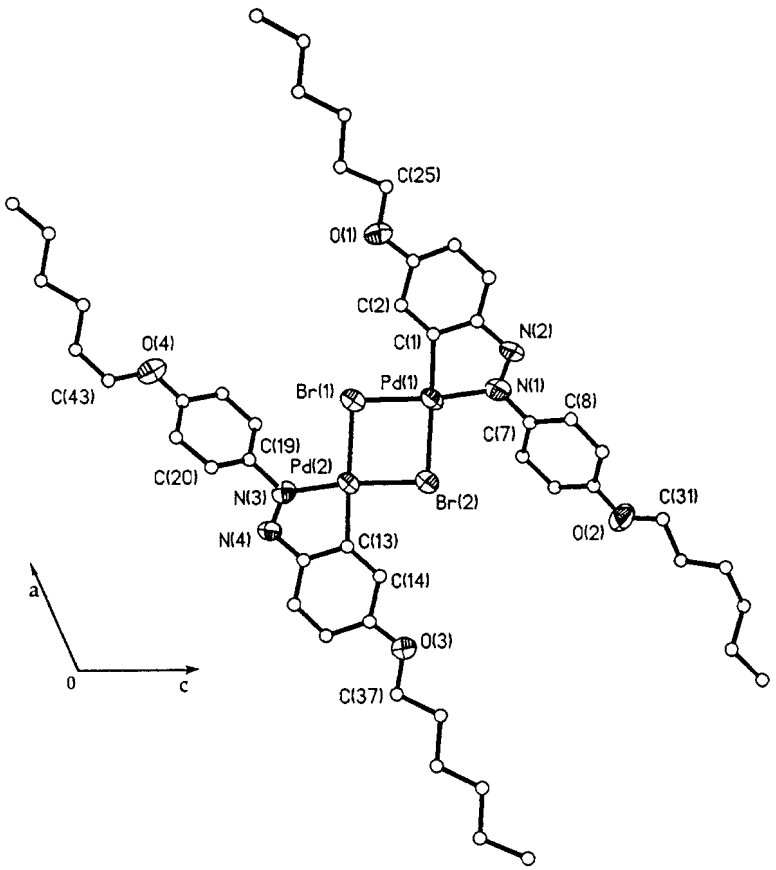

Figure 3 A view of complex **2** along the *b*-axis, showing the atomic numbering scheme.

seems reasonable to suggest an arrangement (Fig. 1) where both the palladium atoms are linked to a planar oxalate ligand to give two five-membered rings.[22]

In summary, as far as the electronic effects of the ligands are concerned, it is worth noting that, along the series **1–3**, the NMR signal of the proton H^3 progressively moves downfield (from 6.83 ppm for **1**, X = Cl, to 7.36 ppm for **3**, X = I; Table 1) as the electron-withdrawing power of the X bridging ligand decreases. Therefore, excluding the ligands with π-electrons close to H^3 (namely N_3 and SCN) the position of H^3 in **7** (6.78 ppm) suggests that the oxalate group exerts an electron-withdrawing power greater than that of Cl.

Crystal structure of complexes 2 and 3

Compounds **2** and **3** crystallize as discrete molecules, each of them being bis(μ-halo)-cyclopalladated complexes. They both crystallize in the monoclinic space group $P2_1/c$, and because they are isomorphous the molecular structure of only the bis(μ-bromo)-cyclopalladated complex **2** is shown in Fig. 3.

Crystal data and relevant refinement parameters are summarized in Table 2. The final coordinates and equivalent isotropic temperature factors of non-H atoms for **2** and **3** are reported in Table 3 and Table 4, respectively.

The two Pd(II) centers in each compound are bridged by the X atoms (X = Br, I). Two cyclometalated azobenzene ligands complete the square-planar coordination sphere. The palladated phenyl rings are found in a *trans* geometry with respect to the Pd–Pd vector. The two five-membered palladacycles in complexes **2** and **3** show essentially the same bond distances and angles (Table 5). These values are also found to be in good agreement with

Table 2 Crystal data and structure refinement for complexes **2** and **3**

Compound	**2**	**3**
Empirical formula	$C_{48}H_{66}Br_2N_4O_4Pd_2$	$C_{48}H_{66}I_2N_4O_4Pd_2$
Formula weight	1135.7	1229.6
Temperature	298 K	298 K
Wavelength	0.71073 Å	0.71073 Å
Crystal system	Monoclinic	Monoclinic
Space group	$P2_{1/c}$	$P2_{1/c}$
Unit cell dimensions	a = 18.925(7) Å	a = 18.967(4) Å
	b = 15.477(5) Å	b = 15.662(5) Å
	c = 18.303(5) Å	c = 18.460(3) Å
	β = 114.18(3)°	β = 113.31(2)°
Volume	4891(3) Å^3	5036(2) Å^3
Z	4	4
Density (calculated)	1.542 g cm^{-3}	1.622 g cm^{-3}
Absorption coefficient	2.415 mm^{-1}	1.984 mm^{-1}
F(000)	2304	2448
θ range for data collection	1.5–25°	1.5–25°
Index ranges	$-22 \leq h \leq 20$, $0 \leq k \leq 18$	$-22 \leq h \leq 20$, $0 \leq k \leq 18$
	$0 \leq l \leq 21$	$0 \leq l \leq 21$
Independent reflections	8553 [R(int) = 0.058]	8888 [R(int) = 0.027]
Observed reflections [$I > 2\sigma(I)$]	3449	2603
Transmission factors	0.455/0.722	0.714/0.907
Number of parameters	301	301
Final R indices[a,b]	R = 0.0771, R' = 0.0642	R = 0.0625, R' = 0.0605
Goodness-of-fit	2.19	1.09
Largest and mean Δ / σ	0.077, 0.003	0.009, 0.001
Largest diff. peak and hole	1.58 and -0.82 e Å^{-3}	0.97 and -0.82 e Å^{-3}

[a] $R = \sum \| \| F_0 \| - \| F_0 \| \| / \sum \| F_0 \|$.
[b] $R' = [\sum \omega (\| F_0 \| - \| F_0 \|)^2 / \sum \omega \| F_0 \|^2]^{1/2}$.

those observed for the previous described isomorphous chloro-bridged complex.[8]

Comparing **2** and **3**, different bond distances are observed within the Pd_2X_2 rhombus. The difference in Pd–X bond length values takes into account either the *trans* influence exerted by the Pd–C(Ar) σ-bond or the size of the halide X. Both Pd_2X_2 rings exhibit a slight folding and the dihedral angles are 13.0(2)° for complex **2** and 12.8(1)° for complex **3**. In similar $[(L')Pd(\mu\text{-}X)]_2$ complexes (HL' = 2,6-dimethylazobenzene; X = Br, I) the folding of the Pd_2X_2 ring has been found to be more pronounced [X = Br: 15.1(1)°; X = I: 19.8(1)°].[23] Accordingly, the intramolecular Pd–Pd separations of 3.674(2) Å for complex **2** and 3.890(2) Å for complex **3** are longer than the corresponding distances found in $[(L')Pd(\mu\text{-}X)]_2$ [X = Br: 3.589(3) Å; X = I: 3.790(1) Å].

While the two orthometalated phenyl rings are essentially coplanar with the respective metallocycles, the two rotationally free phenyl rings break the planarity of the whole molecule. Indeed, the two mean torsion angles N-N-C(ar)-C(ar) are found to be 36(2)° and 39(2)° in **2** and 41(3)° and 40(3)° in **3**. The values of the tilt angles increase along the series X = Cl, Br, I (tilt angles of 35(1)° and 39(1)° for the chloro-bridged derivative), reflecting the steric repulsion involving the X atoms, which increases with the size of the bridging ligand. However, the deviations from planarity are less pronounced than for $[(L')Pd(\mu\text{-}X)]_2$ complexes in which the presence of two bulky methyl groups in *ortho* positions gives tilt angles between 100° and 85°.

The centrosymmetrically related molecules tend to pair. The shortest intermolecular Pd–Pd nonbonded separation (d) is 3.672(2) Å in complex **2** and 3.758(3) Å in complex **3**. The value of d [3.668(1) Å for the chloro-bridged derivative[8]] increases with the size of the halogen-bridged ligand in the order Cl <Br <I. Moreover, since the Pd–Pd intramolecular separations (D) in [(Azo-

Table 3 Atomic coordinates ($\times 10^4$) and equivalent isotropic displacement coefficients ($\text{Å}^2 \times 10^3$) for complex **2**

	x	*y*	*z*	*U*(eq)[a]
Pd(1)	1680(1)	1215(1)	1956(1)	53(1)
Pd(2)	179(1)	1150(1)	−102(1)	51(1)
Br(1)	1662(1)	1306(1)	615(1)	66(1)
Br(2)	198(1)	1330(1)	1232(1)	68(1)
N(1)	1849(7)	1224(8)	3130(7)	54(6)
N(2)	2528(7)	1332(9)	3656(7)	65(6)
N(3)	5(7)	1056(8)	−1272(7)	47(6)
N(4)	−690(7)	1051(8)	−1809(7)	54(6)
O(1)	4643(6)	1215(8)	2327(6)	82(6)
O(2)	−457(6)	899(9)	4246(7)	92(7)
O(3)	−2780(5)	1146(8)	−449(6)	75(6)
O(4)	2214(6)	945(8)	−2551(7)	79(6)
C(1)	2843(8)	1264(11)	2486(8)	55(4)
C(2)	3367(8)	1183(10)	2182(8)	56(4)
C(3)	4156(9)	1277(12)	2702(9)	60(5)
C(4)	4414(9)	1353(11)	3515(9)	68(5)
C(5)	3852(9)	1415(10)	3823(9)	74(5)
C(6)	3070(9)	1351(11)	3311(9)	65(5)
C(7)	1248(8)	1222(11)	3419(8)	44(4)
C(8)	1292(8)	1713(10)	4076(8)	54(4)
C(9)	719(9)	1617(11)	4331(9)	62(5)
C(10)	116(9)	1026(11)	4005(9)	60(5)
C(11)	75(9)	549(11)	3359(9)	65(5)
C(12)	650(8)	612(10)	3077(9)	59(5)
C(13)	−958(8)	1123(10)	−617(8)	45(4)
C(14)	−1506(8)	1155(10)	−321(9)	55(4)
C(15)	−2303(9)	1115(12)	−827(9)	63(5)
C(16)	−2550(8)	1001(9)	−1664(8)	50(4)
C(17)	−2007(8)	1004(10)	−1962(8)	54(4)
C(18)	−1215(9)	1061(11)	−1473(9)	55(4)
C(19)	595(8)	1086(10)	−1588(8)	42(4)
C(20)	472(8)	1546(9)	−2249(8)	52(4)
C(21)	1017(8)	1550(10)	−2589(8)	52(4)
C(22)	1675(9)	1029(11)	−2249(9)	59(5)
C(23)	1773(9)	544(11)	−1588(9)	66(5)
C(24)	1249(8)	581(10)	−1247(9)	54(4)
C(25)	5468(8)	1369(11)	2798(8)	63(5)
C(26)	5849(9)	1367(12)	2220(9)	76(5)
C(27)	6719(8)	1508(11)	2626(9)	67(5)
C(28)	7126(9)	1578(12)	2078(9)	84(6)
C(29)	7994(9)	1629(12)	2496(10)	84(6)
C(30)	8386(11)	1842(13)	1959(10)	117(8)
C(31)	−472(9)	1359(12)	4872(10)	84(6)
C(32)	−1241(11)	1060(14)	4924(13)	134(9)
C(33)	−1431(17)	1420(19)	5495(17)	251(17)
C(34)	−2142(13)	992(18)	5613(15)	195(13)
C(35)	−2813(13)	1333(18)	5083(15)	184(12)
C(36)	−3396(11)	974(13)	5409(11)	125(8)
C(37)	−3587(9)	1099(11)	−915(9)	72(5)
C(38)	−3983(8)	1257(11)	−361(9)	73(5)
C(39)	−4858(8)	1180(11)	−782(8)	70(5)
C(40)	−5243(9)	1334(11)	−216(9)	80(5)
C(41)	−6113(9)	1261(13)	−592(10)	90(6)
C(42)	−6483(11)	1425(13)	3(11)	139(9)
C(43)	2071(11)	1307(14)	−3280(12)	114(7)
C(44)	2633(12)	1085(17)	−3650(13)	166(11)
C(45)	3374(11)	1304(15)	−3184(12)	133(8)
C(46)	3873(11)	1142(15)	−3709(12)	137(9)
C(47)	4665(11)	1325(16)	−3237(12)	152(10)
C(48)	5225(11)	1170(13)	−3610(11)	127(8)

[a] Equivalent isotropic *U* defined as one-third of the trace of the orthogonalized U_{ij} tensor.

Table 4 Atomic coordinates ($\times 10^4$) and equivalent isotropic displacement coefficients ($\mathring{A}^2 \times 10^3$) for complex **3**

	x	*y*	*z*	*U*(eq)
Pd(1)	1735(1)	1186(1)	1996(1)	54(1)
Pd(2)	182(1)	1153(1)	−150(1)	51(1)
I(1)	1734(1)	1293(1)	595(1)	59(1)
I(2)	185(1)	1325(1)	1244(1)	61(1)
N(1)	1887(12)	1213(13)	3163(10)	55(10)
N(2)	2565(11)	1327(16)	3668(10)	75(10)
N(3)	33(11)	1055(11)	−1291(10)	42(9)
N(4)	−658(10)	1079(13)	−1842(10)	49(9)
O(1)	4698(9)	1221(14)	2365(10)	96(10)
O(2)	−423(10)	837(12)	4246(10)	82(10)
O(3)	−2785(9)	1166(14)	−499(10)	85(10)
O(4)	2238(11)	892(12)	−2594(12)	92(11)
C(1)	2871(13)	1218(16)	2523(13)	55(7)
C(2)	3457(15)	1141(17)	2231(15)	68(8)
C(3)	4210(16)	1258(19)	2744(15)	68(8)
C(4)	4478(17)	1391(18)	3537(15)	86(9)
C(5)	3888(16)	1419(16)	3853(16)	89(9)
C(6)	3122(15)	1295(18)	3353(14)	67(8)
C(7)	1288(14)	1130(17)	3447(13)	52(7)
C(8)	1291(13)	1690(15)	4079(13)	54(7)
C(9)	728(13)	1606(15)	4331(13)	56(7)
C(10)	162(15)	1002(16)	4015(15)	58(7)
C(11)	141(15)	471(16)	3397(14)	68(8)
C(12)	719(13)	558(16)	3133(13)	57(7)
C(13)	−964(14)	1141(16)	−673(13)	60(8)
C(14)	−1531(14)	1215(17)	−383(14)	57(7)
C(15)	−2327(15)	1142(18)	−891(14)	60(7)
C(16)	−2537(12)	1049(13)	−1694(12)	44(6)
C(17)	−1976(12)	1030(14)	−2009(13)	47(6)
C(18)	−1193(14)	1089(17)	−1481(14)	60(7)
C(19)	625(13)	1080(15)	−1601(12)	41(6)
C(20)	544(14)	1564(15)	−2266(13)	61(7)
C(21)	1077(15)	1535(18)	−2580(15)	79(9)
C(22)	1688(14)	1004(16)	−2283(14)	55(7)
C(23)	1775(15)	502(17)	−1640(14)	66(8)
C(24)	1257(14)	523(16)	−1280(14)	61(7)
C(25)	5493(13)	1362(19)	2819(14)	72(8)
C(26)	5897(15)	1411(20)	2254(15)	90(10)
C(27)	6774(14)	1501(18)	2661(14)	84(9)
C(28)	7176(14)	1629(18)	2092(15)	82(9)
C(29)	8025(14)	1669(18)	2513(15)	84(9)
C(30)	8462(17)	1858(20)	2017(16)	121(12)
C(31)	−492(15)	1326(20)	4862(16)	95(9)
C(32)	−1271(16)	1021(20)	4858(18)	121(12)
C(33)	−1427(22)	1500(26)	5460(22)	202(20)
C(34)	−2119(22)	1054(29)	5580(25)	223(22)
C(35)	−2853(21)	1337(31)	5072(25)	237(25)
C(36)	−3409(18)	925(22)	5387(18)	145(15)
C(37)	−3594(14)	1128(18)	−964(14)	74(8)
C(38)	−3957(14)	1258(19)	−388(14)	80(8)
C(39)	−4843(15)	1165(18)	−808(15)	87(9)
C(40)	−5256(17)	1282(23)	−248(17)	120(11)
C(41)	−6107(16)	1240(22)	−626(16)	108(10)
C(42)	−6452(18)	1412(22)	−26(18)	146(14)
C(43)	2121(18)	1296(22)	−3296(17)	117(11)
C(44)	2676(17)	1029(24)	−3656(19)	159(16)
C(45)	3449(18)	1339(24)	−3166(18)	144(14)
C(46)	3904(18)	1181(26)	−3711(20)	171(17)
C(47)	4713(19)	1317(29)	−3220(20)	200(20)
C(48)	5232(18)	1198(23)	−3652(17)	150(15)

[a] Equivalent isotropic *U* defined as one-third of the trace of the orthogonalized U_{ij} tensor.

Table 5 Selected bond lengths (Å) and angles (°) for complexes **2** and **3**

	2	**3**
Pd(1)–X(1)	2.443 (2)	2.590 (3)
Pd(1)–X(2)	2.572 (2)	2.718 (3)
Pd(2)–X(1)	2.578 (2)	2.721 (2)
Pd(2)–X(2)	2.442 (2)	2.585 (3)
Pd(1)–N(1)	2.040 (12)	2.059 (20)
Pd(1)–C(1)	2.010 (14)	1.983 (22)
Pd(2)–N(3)	2.035 (13)	2.018 (20)
Pd(2)–C(13)	1.965 (13)	1.998 (23)
N(1)–N(2)	1.263 (14)	1.268 (25)
N(1)–C(7)	1.436 (22)	1.433 (39)
N(2)–C(6)	1.408 (25)	1.395 (40)
N(3)–N(4)	1.280 (14)	1.302 (22)
N(3)–C(19)	1.454 (23)	1.449 (36)
N(4)–C(18)	1.365 (24)	1.418 (38)
C(1)–C(6)	1.397 (22)	1.381 (34)
C(13)–C(18)	1.442 (20)	1.381 (34)
X(1)-Pd(1)-X(2)	85.1 (1)	85.0 (1)
X(1)-Pd(2)-X(2)	85.0 (1)	85.0 (1)
X(1)-Pd(1)-N(1)	171.7 (4)	171.2 (6)
X(2)-Pd(1)-N(1)	102.0 (4)	102.0 (6)
X(1)-Pd(1)-C(1)	92.6 (5)	93.5 (8)
X(2)-Pd(1)-C(1)	173.6 (5)	173.8 (7)
X(1)-Pd(2)-N(3)	102.4 (4)	102.1 (6)
X(2)-Pd(2)-N(3)	171.9 (4)	172.6 (6)
X(1)-Pd(2)-C(13)	175.5 (4)	175.7 (7)
X(2)-Pd(2)-C(13)	92.7 (5)	93.2 (8)
N(1)-Pd(1)-C(1)	79.8 (6)	79.1 (10)
N(3)-Pd(2)-C(13)	79.6 (6)	79.6 (9)

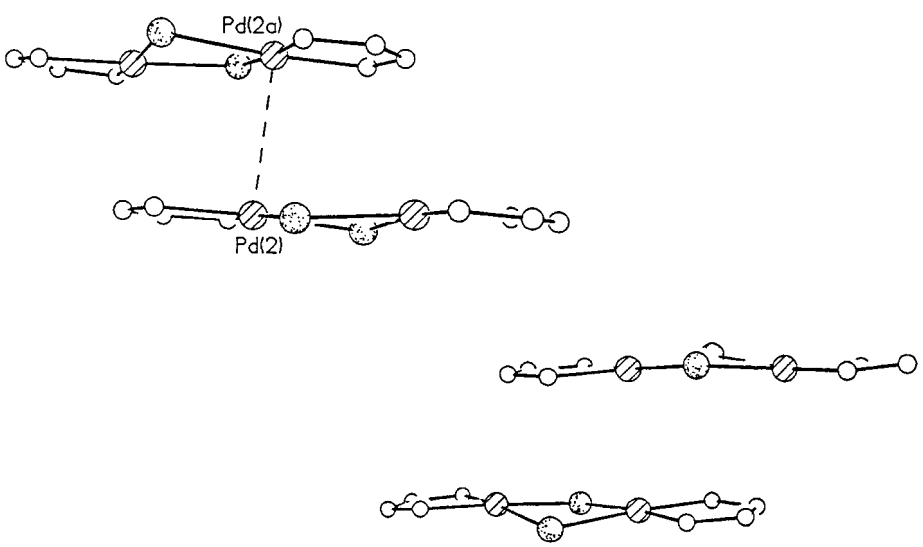

Figure 4 Packing projection for complex **2** viewed down the *a*-axis showing the pair of molecules. Aromatic rings and hexyloxy chains are omitted for clarity.

Table 6 Optical, thermal and thermodynamic data for complexes **1–7**

Compound	Transition[a]	T(° C)	$\Delta H(kJ\ mol^{-1})$
1[c]	C–N	213	42.6
	N–S_E	221	0.75
	S_E–I_{dec}	235	
2	C–I	215	39.0
	I–N	196	0.5
	N–C	190	31.1
3	C–I	211[b]	
4	C–C	150[b]	39.6
	C–S_A	186	5.1
	S_A–I_{dec}	190	
5	C–I	220[a]	
6	C–I	140[a]	
7	C–C	154	45.5
	C–N	238	44.6
	N–S_A	246	4.5
	S_A–I_{dec}	290	

[a] C, crystal; S, smectic; N,nematic; I,isotropic liquid; dec., decomposition. Data recorded during the first heating cycle.
[b] Observed by means of polarized light microscopy only.
[c] Ref. 8.

6)Pd(μ-X)]$_2$ complexes are 3.528(1), 3.674(2) and 3.890(2) Å for X = Cl, Br, I respectively, the *D/d* ratio increases in the same order.

The molecules in the pair are superimposed along the *b*-axis and shifted by nearly 4 Å along the molecular short axis (Fig. 4).

Mesomorphism

These dinuclear palladium complexes display thermotropic mesophases when the bridging group is Cl, Br, N_3 or Ox (compounds **1, 2, 4** and **7**, respectively). The liquid-crystalline behavior of **1** was discussed in a previous paper,[8] so here we briefly describe the mesomorphism of **2, 4** and **7** only. The mesophases they exhibit were identified by the optical textures observed by polarizing microscope[24] and confirmed by XRD analysis performed on powder samples. The transition temperatures and enthalpies, determined by DSC measurements, are shown in Table 6.

In particular, the thermotropic behavior of the bromo-bridged complex **2** features a monotropic nematic phase, N, showing a Schlieren texture,[24] stable in a rather narrow temperature range (6 °C).

The azide-bridged palladium complex **4**, after a crystal-to-crystal transition at 150 °C, gives rise to a smectic A phase, S_A, between 185.6 and 190.1 °C. This mesophase features a polygonal texture which transforms into a fanshaped texture[24] just before the clearing point at 190 °C (with partial decomposition). XRD measurements agree with the mesomorphism described.

The mesogenic properties are changed significantly by replacing the azide with the oxalate bridge. Indeed complex **7**, in the first heating process, after a change of the crystalline phase at 154 °C, exhibits a mesophase whose nature is not assigned. The structural classification of this mesophase has been omitted because it is controversial. Indeed, both the optical texture and X-ray pattern suggest a nematic phase while it is well known that the disordered N phase has to be expected at a higher temperature than the more ordered S_A mesophase. Moreover, subjecting the sample to a second heating run, the N mesophase does not appear and the S_A phase extends over a temperature range which starts from a temperature lower than that at which it appeared during the first heating run. Thus, although reproducible in virgin samples, this mesophase is not a permanent property of this material. In order to clarify this point further investigations on similar oxalate complexes are in progress.

Further heating causes isotropization to occur at 290 °C, with partial decomposition. It should be noted that, on cooling the S_A phase, **7** solidifies at 201 °C, keeping the order of the S_A phase until room temperature. The second heating run shows the S_A phase only, which is stable between 225 and

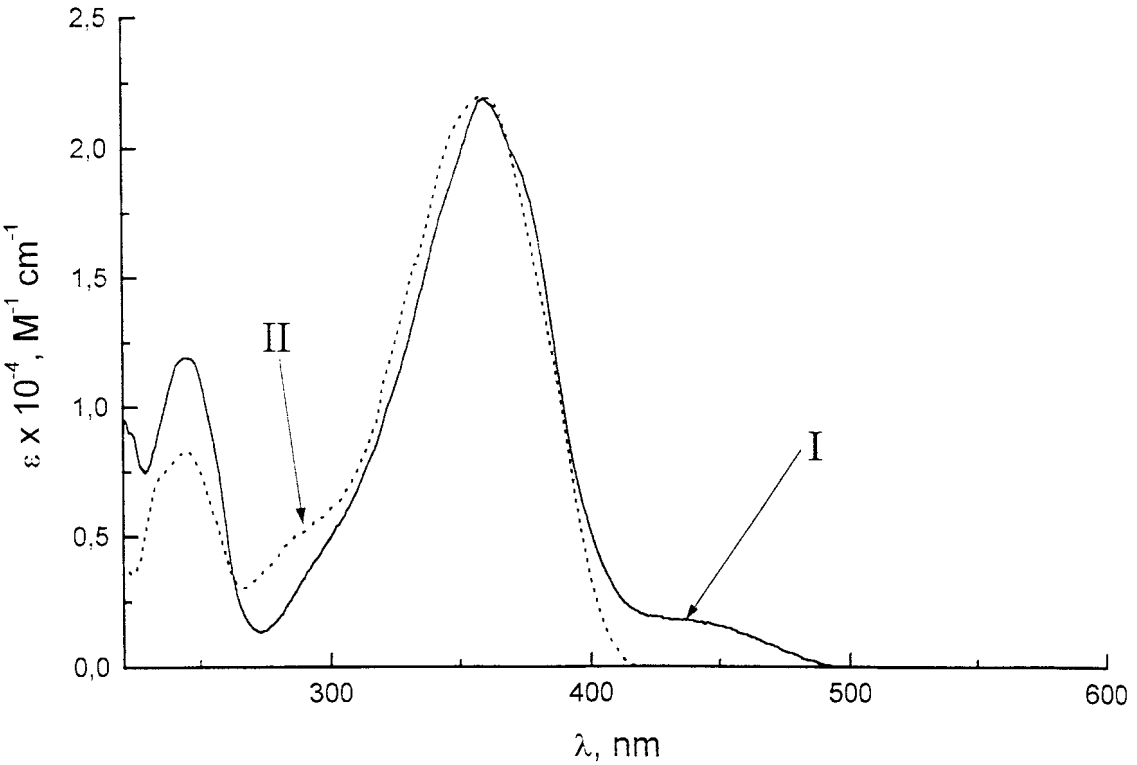

Figure 5 Absorption spectra in CH_2Cl_2 of the uncomplexed ligands **I** and **II**.

287 °C. The nature of this phase was confirmed by variable-temperature X-ray diffraction studies carried out on a powdered sample.

Absorption spectra

The optical properties of azobenzenes have been under scrutiny for a long time.[25] The electronic absorption spectra of this type of compounds typically show two low-energy bands. An illustration is provided by Fig. 5, where the absorption spectra of the 4,4′-bis (hexyloxy) azobenzene, [H(Azo-6)], **I**, *trans* isomer (Fig. 2), and of the 4,4′-bis (hexyloxy) azobenzene, [H(Azoxy-6)], **II**, are compared.

For ligand **I**, the two lowest-energy absorption bands peak at 359 and 441 nm, with extinction coefficients ε = 22000 and 1700 M^{-1} cm^{-1}, respectively. The more intense higher-energy band is associated with a transition connecting the ground and $^1\pi\pi^*$ excited states; the lower-intensity band corresponds to a transition involving n non-bonding orbitals localized on the nitrogen atoms, and leads to direct population of $^1n\pi^*$ excited states.[25] The latter transition cannot take place for **II**, because the electrons residing in the n orbitals are engaged in the bond to the oxygen atom (Fig. 2). Accordingly, the absorption spectrum for **II** does not exhibit the weak band around 440 nm (Fig. 5).

The *trans–cis* photoisomerization exhibited by the flexible azo group has been one of the most studied reactions in the field of organic photochemistry.[25,26] A convenient description of the process may be given in terms of the potential energy curves for the lowest-lying excited states.[27,28] The thermally stable *trans* configuration, and the *cis* configuration that these compounds can assume under photoirradiation, are characterized by shallow minima for singlet and triplet levels (both of $\pi\ \pi^*$ and $n\pi^*$ electronic nature), as a function of the *trans–cis* nuclear coordinate. As a consequence, the non-radiative processes (which include the *trans–cis* interconversion), deactivating the excited states, are very fast and compete efficiently with the radiative process. A lack of any practically detectable luminescence for the azobenzenes results.

For some azobenzene cyclometalated mono-

Table 7 Spectroscopic and photophysical data[a]

Compound	Absorption, λ (ε M^{-1}cm^{-1})	Color	Emission		
			λ_{max}[b] (nm)	τ (ns)	$\phi \times 10^4$[c]
1	258 (32 000); 375 (22 000); 472 (22 000)	Yellow	536	3.4	0.9[d]
2	268 (52 000); 371 (31 000); 472 (27 000)	Yellow	522	4.6	0.85
3	268 (52 000); 372 (28 000) 467 (19 000)	Orange	522	4.6	0.8
4	265 (82 000); 378 (35 000); 475 (30 000)	Orange	578	1.2	46.8
5	260 (35 000); 373 (22 000); 465 (21 000)	Dark red	574	0.96	2.5
6	262 (26 000); 371 (28 000); 467 (27 000)	Purple	552	3.49	1.4
7	260 (19 000); 377 (14 700); 480 (17 500)	Orange–yellow	582	0.4	2.0
I	243 (12 000); 359 (22 000); 441 (1 700)	Pale yellow	—	—	—
II	243 (12 000); 363 (22 000); —	Yellow	—	—	—
Ib	229 (31 000); 376 (12 400); 475 (15 000)	Pale yellow	560	1.7	4.7[d]
IIa	230 (59 000); 329 (32 000); 433 (15 000)	Pale yellow	—	—	—
IIb	231 (36 000); 320 (17 000); 426 (11 400)	Orange–yellow	—	—	—

[a] Solvent CH_2Cl_2, room temperature.
[b] For uncorrected spectra.
[c] From corrected spectra; see Experimental section.
[d] Ref. 9b.

nuclear Pd(II) complexes we have already shown that luminescence can be observed.[9b] This is due to the blocking of the azo group in the *trans* configuration as a consequence of the formation of a five-membered ring involving the metal center.

Table 7 collects the spectroscopic results and the photophysical data for the reference azo ligand **I**, its dinuclear **1–7** and mononuclear **Ia** derivatives and the reference azoxy ligand **II** together with the its complexes **IIa** and **IIb**. Selected absorption spectra for the dinuclear complexes **1–7** are shown in Fig. 6. Worthy of note is the fact that these spectra are characterized by closely overlapping profiles, with the exception of compound **6**.

In particular, all the complexes exhibit two broad band systems in the violet–visible wavelength region. The higher-energy bands peak at 350–380 nm and compare well with the intense band for the parent ligand **I**, which peaks at 359 nm. On this basis, for complexes **1–5** and **7** the band at around 350–380 nm is assigned to an intraligand $\pi\pi^*$ origin, similar to the case of the reference ligand **I** and of the related mononuclear complex **Ib** (Table 7).[9b]

For complexes **1–5** and **7**, the quite intense band peaking at around 470 nm, ($\varepsilon > 10^4$ M^{-1} cm^{-1}), which imparts the color these species show, does not find a similar counterpart in **I**, where only a very weak band (ε 10^3 M^{-1} cm^{-1}) is present at 441 nm. Comparison between the spectra for complex **IIa** and the corresponding ligand **II** reveals even more clearly that the band at 433 nm for the former is not observed at all in the latter, thus confirming that this type of band finds its origin in electronic transitions occurring within the complexes but is absent within the uncomplexed ligands. In addition, the data collected in Table 7 show that the energy position of lowest-energy band in the dinuclear complexes is affected somewhat both by the nature of the bridge and by the presence of the azo or the azoxy group. These observations suggest that the intense, lowest-energy, absorption band recorded for the palladium complexes is related to the electronic properties of the five-term ring, i.e. the cyclopalladated ring. According to a simplified description in terms of MO energy levels, the low energy for this transition might be related to the presence of an electron residing in an MO which should correspond to the LUMO for the related non-cyclometalated aromatic ring.[9]

Spectroscopy and structural properties

As previously discussed, a substantially symmetric structure can be assumed for the dinuclear species **1–5** (X = Cl, Br, I, N_3, SCN) and **7** (X = Ox). This is in agreement with the fact that the absorption spectra of the complexes closely resemble each other (Fig. 6).

One remarkable exception to this behavior occurs for complex **6** where the bridging group is

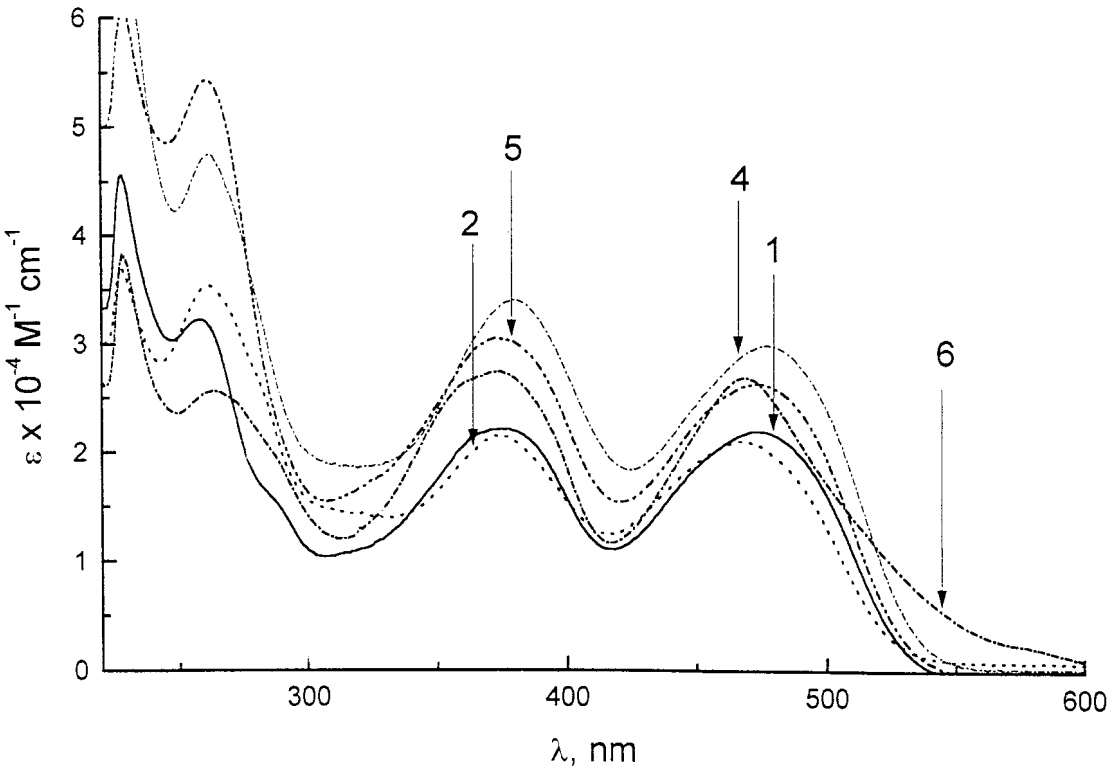

Figure 6 Absorption spectra in CH_2Cl_2 of some representative examples of dinuclear complexes $[(Azo\text{-}6)Pd(\mu\text{-}X)]_2$.

acetate. The suggested molecular structure of this complex is bent, with the two azobenzene moieties kept at a close distance with a Pd–Pd separation of about 3 Å (Ref. 21; see also A. Crispini and M. Ghedini, Comments Imorg. Chem. (1999), in press). This arrangement is thought to cause a high degree of interaction between the aromatic rings, as reported for other constrained systems.[29] As a consequence the long tail on the red side of the lowest-energy absorption band of **6** (Fig. 6) may be ascribed to such an interaction and is therefore thought to be responsible for the violet color exhibited by **6**.

Luminescence spectra

The data gathered in Table 7 show that while the palladium azoxybenzene complexes **IIa** and **IIb** are not luminescent, most azobenzene complexes give luminescence.

This may be of importance for two reasons. First, some practical use of the luminescence (even if it is weak, as in this case) may be envisaged for applications requiring film-forming materials.[30] Second, the determination of the energy level for the emissive excited state may allow the positioning of the energy level of the lowest-lying excited states for azobenzene compounds.[25,27,28] For instance, concerning the latter point we have seen that the *trans* blocking of the azo group occurring in cyclometalated dinuclear complexes results in an intense absorption band centered at around 470 nm and an emission band centered at around 560 nm, which can be ascribed to excited states of the cyclopalladated ring of an $n\pi^*$ nature.[9] This amounts to an apparent Stokes shift of about 2000 cm^{-1}. Thus, given that the transition from the ground state to the $^1n\pi^*$ level of ligand **I** (the lowest-lying level for the *trans* configuration) may be positioned at 2.8 ev based on the absorption data, the corresponding *trans*-$^1n\pi^*$ relaxed level could be roughly placed at 2.5–2.6 eV, provided the same value for the Stokes shift can be assumed. Similarly, for the relaxed *trans*-^{1} $\pi\pi^*$ level it would provide an energy of 3.2–3.3 eV. It seems therefore that, while sensitization of the triplet level has been

used for the determination of the various triplet energies for azobenzene-like compounds,[31] this approach might be of help in evaluating the energy layout for their singlet excited states.

CONCLUSIONS

The synthesis of the series of bridged dinuclear cyclopalladated complexes **1–7** was successfully achieved. Single-crystal X-ray analysis of the dinuclear bromo- and iodo-bridged complexes has been performed. The structural data, compared with those of the homologous chloro compound, show that all the $[(Azo\text{-}6)Pd\ \mu\text{-}X)]_2$ (X = Cl, Br, I) molecules crystallize in the monoclinic space group $P2_1/c$ and are isomorphous. They are arranged in slipped pairs with intermolecular non-bonding Pd–Pd contacts ranging from 3.668(1) Å (X = Cl) to 3.758(3) Å (X = I). The electronic and geometric properties of the reacted bridging ligands impose different intramolecular Pd–Pd separations. In particular, the X-ray crystal structure determinations of **1–3** give the following Pd–Pd distances: **1** = 3.528(1) Å,[8] **2** = 3.674(2) Å, **3** = 3.890(2) Å, whereas the analogous distances found in complexes similar to **4–7** are 3.283(1), 5.575(3), 3.196(3) Å (A. Crispini and M. Ghedini, Comments Inorg. Chem. (1999), in press) and 5.462(2) Å.[22] Keeping in mind the molecular geometries of complexes **1–3** and those proposed above for **4–7**, the planar $Pd(\mu\text{-}X)_2Pd$ (X = Cl, Br, I, N_3, SCN) and $Pd_2(Ox)$ fragments can be compared. Thus, it is apparent that the bridging SCN groups (complex **5**) force the two palladium atoms to maintain a distance which is comparable with that estimated for the bis-chelating oxalate group (complex **7**) and about 2 Å larger than for Cl, Br, I or N_3 (complexes **1–4**). The investigations into their thermal behavior show that, by changing the bridging group X, dramatic differences occurred. In particular, the data obtained by this comparative study indicate that liquid-crystalline properties are depressed for iodide (**3**), thiocyanate (**5**) or acetate (**6**), whereas they are promoted for chloride (**1**), bromide (**2**), azide (**4**) or oxalate (**7**) bridges (Table 6). Remarkably, with reference to the synthesis of new palladium mesogens, compound **7** is the first example reported until now of an 'H-shaped' species containing the bridging oxalate group.

As far as the spectroscopic properties of **1–7** are concerned, for the examined complexes the lowest-energy absorption band is most likely to be associated with electronic transitions localized on the cyclopalladated ring. This interpretation is supported by the fact that the characteristics of this band (energy position and intensity) appear to be sensitive to changes occurring in the electronic environment of the cyclopalladated ring; an illustration is provided through Fig. 6, where the absorption spectra for **1, 2, 4, 5** and **6** are compared. For instance, the presence of the oxalate group seems to reduce the absorption properties whereas the azide group significantly increases the luminescence efficency (Table 7). From the point of view of possible applications, an useful outcome is that the range of observed colors for the investigated compounds changes from pale yellow (**1**) to orange (**4**), dark red (**5**) and violet (**6**). Interestingly, these observations may be exploited for achieving a certain degree of color tuning in this type of material.

Acknowledgements Financial support from the Italian Ministero per l'Universita' e la Ricerca Scientifica e Tecnologica (MURST), the Consiglio Nazionale delle Ricerche (CNR) and the Regione Calabria (POP 1994–99) is gratefully acknowledged.

REFERENCES

1. L. M. Blinov and V. G. Chigrinov, *Electrooptic Effects in Liquid Crystal Materials*, Springer, New York, 1994.
2. I. C. Khoo, *Liquid Crystals: Physical Properties and Nonlinear Optical Phenomena*, Wiley, New York, 1995.
3. G. P. Wiederrecht, B. A. Yoon, W. A. Svee and M. R. Wazielewski, *J. Am. Chem. Soc.* **119**, 3358 (1997).
4. S. H. Chen, H. Shi, B. M. Conger, J. C. Mastrangelo and T. Tsutsui, *Adv. Mater.* **8**, 998 (1996).
5. M. Grell, D. D. C. Bradley, M. Inbasekaran and P. E. Woo, *Adv. Mater.* **9**, 798 (1997).
6. Serrano, J. L. (ed.), *Metallomesogens*, VCH, Weinheim, 1995.
7. A. M. Levelut, M. Veber, O. Francescangeli, S. Melone, M. Ghedini, F. Neve, F. P. Nicoletta and R. Bartolino, *Liq. Cryst.* **19**, 241 (1995).
8. A. Crispini, M. Ghedini, S. Morrone, D. Pucci and O. Francescangeli, *Liq. Cryst.* **20**, 67 (1996).
9. (a) Y. Wakatsuki, H. Yamazaki, P. A. Grutsch, M. Santhanam and C. Kutal, *J. Am. Chem. Soc.* **107**, 8153 (1985) (b) M. Ghedini, D. Pucci, G. Calogero and F. Barigelletti, *Chem. Phys. Lett.* **267**, 341 (1997).
10. M. Guardigli, L. Flamigni, F. Barigelletti, C. S. W. Richards and M. D. Ward, *J. Phys. Chem.* **100**, 10620 (1996).
11. M. Ghedini, S. Morrone, F. Neve and D. Pucci, *Gazz. Chim. It.* **126**, 1 (1996).

12. A. C. T. North, D. C. Phillips and F. S. Mathews, *Acta Cryst., Sect. A* **24**, 351 (1968).
13. SHELXTL PLUS, Version 4.21, Siemens Analytical X-ray Instruments Inc., Madison, WI, (1990).
14. M. Nardelli, *Comp. Chem.* **7**, 95 (1983).
15. S. Kuang, Z. Zhang, Q. Wang and T. C. W. Mak, *J. Chem. Soc., Dalton Trans.* 4477 (1997).
16. W. P. Fehlhammer and L. F. Dahl, *J. Am. Chem. Soc.* **94**, 3377 (1972).
17. (a) J. Barberà, P. Espinet, E. Lalinde, M. Marcos and J. L. Serrano, *Liq. Cryst.* **2**, 833 (1987) (b) N. Usol'tseva, K. Praefcke, D. Singer and B. Gündogan, *Liq. Cryst.* **16**, 601 (1994).
18. M. A. Ciriano, P. Espinet, E. Lalinde, M. B. Ros and J. L. Serrano, *J. Mol. Struct.* **196**, 327 (1989).
19. R. G. Pearson, *Inorg. Chem.* **12**, 712 (1973).
20. J. Buey and P. Espinet, *J. Organometal. Chem.* **507**, 137 (1996).
21. M. Ghedini, D. Pucci, G. De Munno, D. Viterbo, F. Neve and S. Armentano, *Chem. Mater.* **3**, 65 (1991).
22. T. Kawato, T. Uechi, H. Koyama, H. Kanatomi and Y. Kawanami, *Inorg. Chem.* **23**, 764 (1984).
23. A. Crispini, M. Ghedini and F. Neve, *J. Organometal. Chem.* **448**, 241 (1993).
24. D. Demus and L. Richter, *Textures of Liquid Crystals*, Verlag Chemie, Weinheim, 1978.
25. Dürr, H. and Bouas-Larent, H. (eds), *Photochromism*, Elsevier, Amsterdam, 1990, p. 16, and references therein.
26. For recent contributions, see (a) J. Wachtveil, T. Nägele, B. Puell, W. Zinth, M. Krüger, S. Rudolph-Böhner, D. Oesterhelt and L. Moroder, *J. Photochem. Photobiol. A: Chem.* **105**, 283 (1997) (b) F. Lagugné-Labarthet and C. Sourisseau, *J. Photochem. Photobiol. A: Chem.* **21**, 879 (1997).
27. S. Monti, G. Orlandi and P. Palmieri, *Chem. Phys.* **71**, 87 (1982).
28. H. Rau, *J. Photochem.* **26**, 221 (1984).
29. V. Balzani and F. Scandola, *Supramolecular Photochemistry*, Ellis Horwood, Chichester, 1991, Chapter 9.
30. C. Weder, C. Sarwa, A. Montali, C. Bastiaansen and P. Smith, *Science* **279**, 835 (1998).
31. S. Monti, E. Gardini, P. Bortolus and E. Amouyal, *Chem. Phys. Lett.* **77**, 115 (1981).

